Single-Chip Integrated Electro-Optic Polymer Photonic RF Phase Shifter Array

Jeehoon Han, *Senior Member, IEEE*, Byoung-Joon Seo, SeongKu Kim, Hua Zhang, and Harold R. Fetterman

***Abstract*—This paper demonstrates a four-element integrated photonic radio-frequency (RF) phase shifter array in a single chip with an advanced configuration. These devices are integrated using electrooptic polymer materials and involve several novel technologies. Measurements of this configuration showed that our four outputs were independent and had highly linear RF phases over 360° with negligible RF power fluctuation at the modulation frequency of 20 GHz. This significant improvement is capable of removing one of the major problems in using this type of phase shifter architecture.**

***Index Terms*—Beam-forming systems, optical single sideband (SSB) modulators, phased array antenna, photonic radio-frequency (RF) phase shifters.**

I. Introduction

PHASED array antennas using photonic radio-frequency (RF) phase shifters hold great promise for advanced wireless communications and radar applications due to their many advantages such as simple implementation, optical distribution capability, low cost, light weight, and small size [1]–[6]. They can control multiple RF phases using dc voltages and feed the independent phase outputs into an antenna array to perform rapid and continuous beam-forming functions. Among the possible phase shifter architectures, the one described in [1] is the simplest and most flexible approach. In actual implementation, one can integrate multiple phase shifters in a single chip providing multiple independent phase outputs. Such a phase shifter array can significantly reduce the complexity of RF distribution structures fed by a single RF and optical source. In contrast to microwave monolithic integrated circuit systems, the frequency bandwidth of these devices is very wide and effectively covers from dc to over 50 GHz. Also, it allows continuous beam-forming without limitation on the number of beam angles. This design of the phase shifter, however, suffers from a lack of phase shift linearity and a substantial amount of power variation as the phase is tuned.

Having recognized the requirements for practical usage, we present an advanced configuration for a four-element photonic RF phase shifter array. For these devices, our recently developed polymer materials and advanced fabrication technologies enabled flexible design and integration as well as broad bandwidth operation. Also, we discuss the new generation of phase-shifter architecture using a multimode interference (MMI) structure to further reduce the complexity.

Manuscript received March 18, 2003; revised July 29, 2003. This work was supported in part by AFOSR and DARPA.

J. Han, B.-J. Seo, S. Kim, and H. R. Fetterman are with the Electrical Engineering Department, University of California, Los Angeles, CA 90095 USA (e-mail: hoon@ee.ucla.edu).

H. Zhang was with Pacific Wave Industries, Los Angeles, CA 90024 USA. He is now with the Electrical Engineering Department, University of California, Los Angeles, CA 90095 USA.

Digital Object Identifier 10.1109/JLT.2003.819801

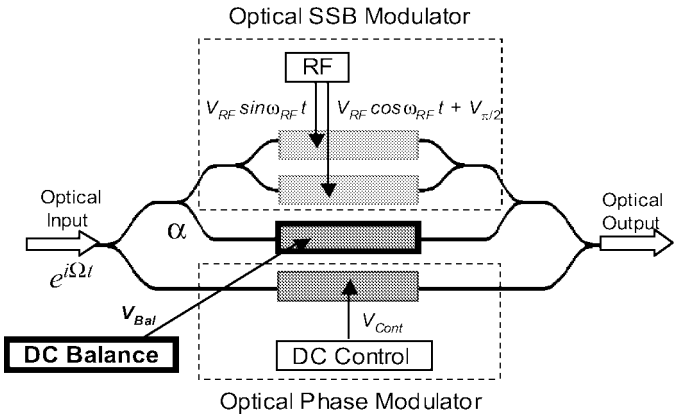

Fig. 1. Schematic diagram representing the balanced photonic RF phase shifter with a balancing arm. α represents the optical power-splitting ratio at the balancing arm.

II. Advanced Photonic RF Phase-Shifter Design

The architecture described in [1], which is analogous to the structure shown in Fig. 1 except for the balancing arm, consists of a single-sideband (SSB) modulator on one arm of a Mach–Zehnder (MZ) and an optical phase modulator on the other arm. The SSB modulator unit generates a carrier at Ω and a sideband at $\Omega+\omega_{\rm RF}$. On the other arm of the MZ, the control dc bias $V_{\rm Cont}$ is applied to the optical phase modulator to induce a phase-shifted optical carrier at Ω. Finally, the mixing of these signals in a photodiode gives rise to the RF signal at $\omega_{\rm RF}$ with a variable phase controlled by $V_{\rm Cont}$.

The calculated RF phase and power characteristics are shown in Figs. 2 and 3 as a function of control voltage at a modulation depth of 0.5. The phase of the RF signal can be controlled by changes in control voltage $V_{\rm Cont}$ and varies almost linearly up to 140°. However, it starts exhibiting a lack of linearity as the control voltage is tuned over $2V_\pi$. A maximum RF phase deviation of approximately 50° from the ideal linear characteristic is observed. In addition, the RF power exhibits fluctuation of approximately 15 dB as the control voltage is tuned over $2V_\pi$. For most practical applications, a wide range of linear phase shifting is required and the RF power fluctuation is very undesirable. Most of the detrimental effects are caused by the presence of the carrier signal from the SSB modulator unit [4]. This carrier signal is added to another phase shifted carrier signal at the same frequency Ω and mixed with the sideband in the photodiode. The resulting RF signal reveals degradation of phase

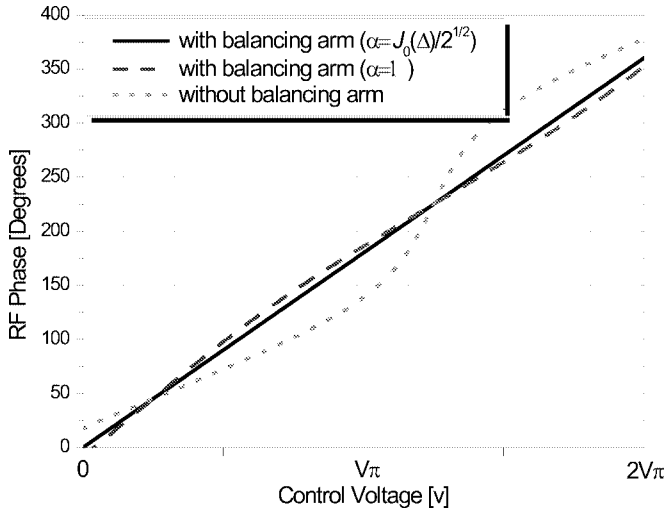

Fig. 2. The calculated RF phase characteristics as a function of control voltage at a modulation depth of 0.5.

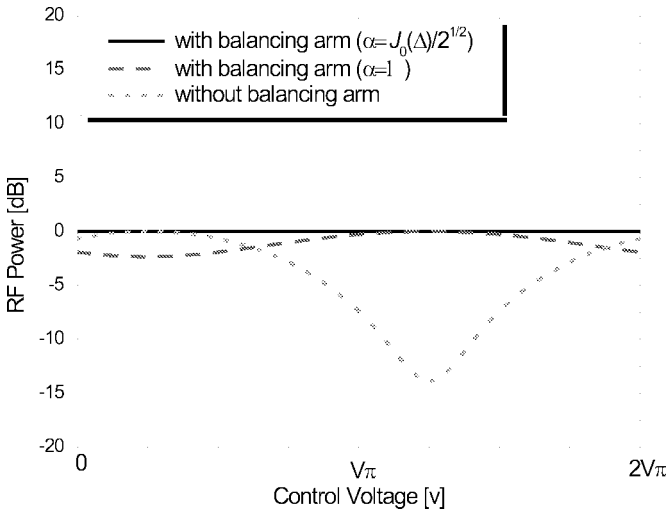

Fig. 3. The calculated RF power characteristics as a function of control voltage at a modulation depth of 0.5 (normalized to each maximum power).

and power characteristics. This effect is even more pronounced as the modulation depth is decreased. Choosing higher modulation depth tends to diminish these effects. This operating condition, however, is unfavorable in that it requires a considerable amount of RF source power and also generates harmonics and signal distortion. As a consequence, an alternative scheme with a reasonable modulation depth is required to extend the range of applications for these devices.

A simple solution has been developed to solve these problems under small signal operation. If the carrier signal is fully suppressed in the SSB modulator, these unwanted effects could be largely eliminated. Fig. 1 represents the schematic diagram for the balanced photonic RF phase shifter. This architecture inserts an additional arm in the inner MZ, which is intended to suppress the carrier signal in the SSB modulator so as to balance the system.

If the input optical signal with unit magnitude at a frequency of Ω is $E_{\rm in}(t) = e^{i\Omega t}$, the output optical field and the resulting intensity at the modulation frequency $\omega_{\rm RF}$ can be expressed as

$$E(t) = \frac{1}{4(1+\alpha)} e^{i\Omega t}\left[e^{i\Delta\sin(\omega_{\rm RF}t)} + e^{i\Delta\cos(\omega_{\rm RF}t)+i\frac{\pi}{2}} + 2\alpha e^{i\phi_{\rm Bal}} + 2(1+\alpha)e^{i\phi_{\rm Cont}}\right] \quad (1)$$

$$I_{\omega_{\rm RF}}(t) = \frac{1}{4(1+\alpha)^2} A_{\rm RF} J_1(\Delta)\cos(\omega_{\rm RF}t + \varphi_{\rm RF}) \quad (2)$$

where

$$A_{\rm RF} = \Big\{\left[J_0(\Delta)+2\alpha\cos\phi_{\rm Bal}+2(1+\alpha)\cos\phi_{\rm Cont}\right]^2 + \left[J_0(\Delta)+2\alpha\sin\phi_{\rm Bal}+2(1+\alpha)\sin\phi_{\rm Cont}\right]^2\Big\}^{\frac{1}{2}} \quad (3a)$$

$$\varphi_{\rm RF} = \tan^{-1}\left[\frac{J_0(\Delta)+2\alpha\sin\phi_{\rm Bal}+2(1+\alpha)\sin\phi_{\rm Cont}}{J_0(\Delta)+2\alpha\cos\phi_{\rm Bal}+2(1+\alpha)\cos\phi_{\rm Cont}}\right]. \quad (3b)$$

Here V_π is the half-wave voltage, $\Delta = \pi V_{\rm RF}/V_\pi$ is the modulation depth, $\phi_{\rm Cont} = \pi\cdot(V_{\rm Cont}/V_\pi)$ is the optical phase shift by the control dc bias, $\phi_{\rm Bal} = \pi\cdot(V_{\rm Bal}/V_\pi)$ is the optical phase shift by the balancing dc bias, and α^2 is the optical power-splitting ratio at the balancing arm. The desired phase and magnitude of the optical signal in the balancing arm are established by the proper dc bias and splitting ratio, respectively.

The calculated RF phase and power characteristics of the balanced structure are shown in Figs. 2 and 3 in comparison with the structure without the balancing arm. For the choice of $\alpha = J_0(\Delta)/\sqrt{2}$ with $\phi_{\rm Bal} = 5\pi/4$, the undesirable terms $J_0(\Delta)$ completely disappear (that is, the carrier signal is fully suppressed in the SSB modulator) and the ideal characteristics for the RF phase and power can be obtained such that

$$A_{\rm RF}^2 = const., \quad \varphi_{\rm RF} = \tan^{-1}\left[\frac{2\sin\phi_{\rm Cont}}{2\cos\phi_{\rm Cont}}\right] = \phi_{\rm Cont}.$$

This indicates that the RF power does not vary at all and the RF phase shift is highly linear with respect to the control dc voltage, which makes these devices very suitable for optically controlled phase array antenna systems.

Assuming a simple symmetric splitting at the balancing arm, i.e., $\alpha = 1$, with $\phi_{\rm Bal} = 5\pi/4$, this system shows a maximum phase deviation of less than 6° while maintaining the RF power fluctuation below 3 dB as the control voltage is tuned over $2V_\pi$. In this case, the carrier suppression in the SSB modulator is only partially accomplished since the balancing power is unequal to the carrier signal from the SSB modulator unit. Nevertheless, this significant improvement of nearly one order of magnitude is capable of removing one of the major problems in using this type of phase shifter architecture.

It is favorable to integrate multiple phase shifters in a single chip. This phase shifter array significantly reduces the complexity of RF feed structures and needs only a single RF and optical source. In a previous work, we have successfully demonstrated a compact two-element photonic RF phase shifter as a first step to development of an array of phase shifters [7]. This basic concept now has been extended to the advanced design in conjunction with the balanced architecture. The four-element phase-shifter array incorporating the balanced design is shown

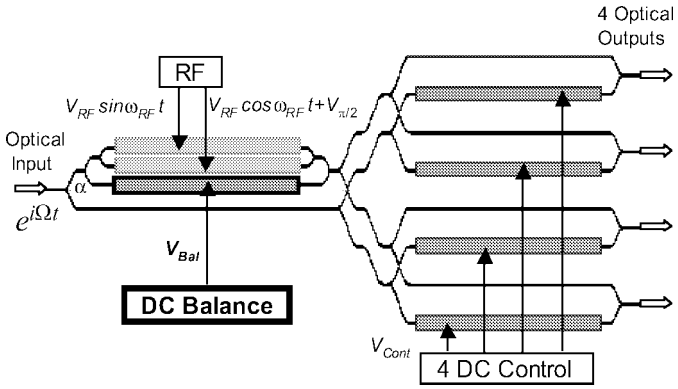

Fig. 4. The schematic diagram for the four-element RF phase shifter array with the balanced design.

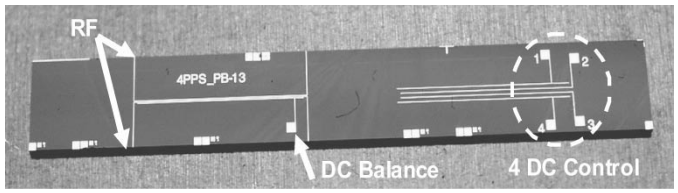

Fig. 5. The balanced multiple output photonic RF phase shifter fabricated in the APC-CPW polymer material.

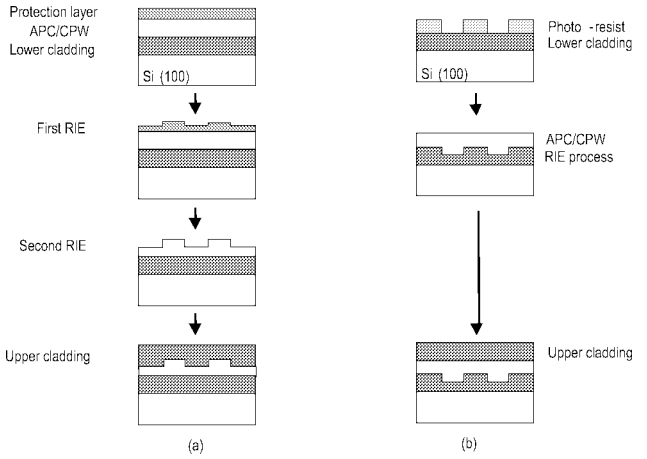

Fig. 6. Comparison of two fabrication procedures in (a) typical rib structures and (b) inverted rib structures.

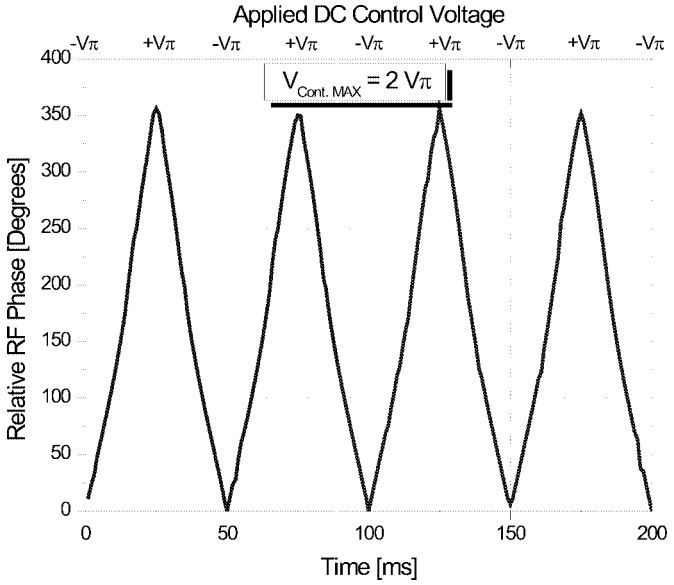

Fig. 7. The measured RF phase from a single output.

in Fig. 4. The modulated optical output from the balanced SSB modulator is split into four branches and combined with the four outputs from the optical phase shifters. This signal distribution in a planar chip was achieved through the use of low crosstalk waveguide crossings and S-bend waveguide structures. The performance of these devices could be severely impacted by that of the optical waveguide crossings, and as such they were carefully implemented.

Fig. 5 shows the phase-shifter array in a single chip fabricated using recently developed polymer materials and advanced polymer fabrication technologies. The device size of the phase shifter with four outputs was 3.8×0.5 cm. For the simplicity of the design, the splitting ratio of the balancing arm α was set to be one. This guest-host system exhibits a high electrooptic coefficient, low material loss at 1.55 μm, and wide-band frequency response over 100 GHz [8]. The single-mode (SM) ridge optical waveguides were fabricated using the new inverted rib structures as shown in Fig. 6. The key benefit of these inverted rib structure is that it can eliminate damage problems of the core layer due to the photoresist solvents and etching processes [9]. This ultimately resulted in much simpler fabrication procedures and lower propagation losses. Also the SM waveguide structures were designed to provide the symmetric mode shape with a rib depth of 0.8 μm and waveguide width of 4 μm. A large optical nonlinearity in the core region was then achieved through the electrode poling. The microstrip lines with a characteristic impedance of 50 Ω were vertically aligned to the optical waveguides in the interaction regions, giving a traveling-wave configuration. For the minimum device length and insertion loss, raised-sine S-bend waveguide structures have been used in all the optical waveguide bending sections [10]. The test structures for the S-bend and waveguide crossings were fabricated on the same wafer. The measured bending losses of the S-bend structures were less than 0.2 dB. The measured excess optical loss due to the crossing was less than 0.5 dB, and the optical waveguide crossings exhibited a crosstalk level of less than -28 dB.

III. Measured Phase-Shifter Performance

The measured RF phase and power of a single element are shown in Figs. 7 and 8 at the modulation frequency of 20 GHz and modulation depth of 0.58. The performance of our phase shifter was measured using the experimental setup shown in Fig. 9. Triggering the HP 8510 network analyzer with the function generator allows the phase and power of the 20-GHz signal to be monitored as a function of time synchronized to the triangular control voltage. The linear relationship between voltage and time in the control triangular waveform enabled a one-to-one mapping between the measured RF phase (or power) and the control dc voltages. Therefore, the control voltage changes by $2V_\pi$ for a period of 25 ms.

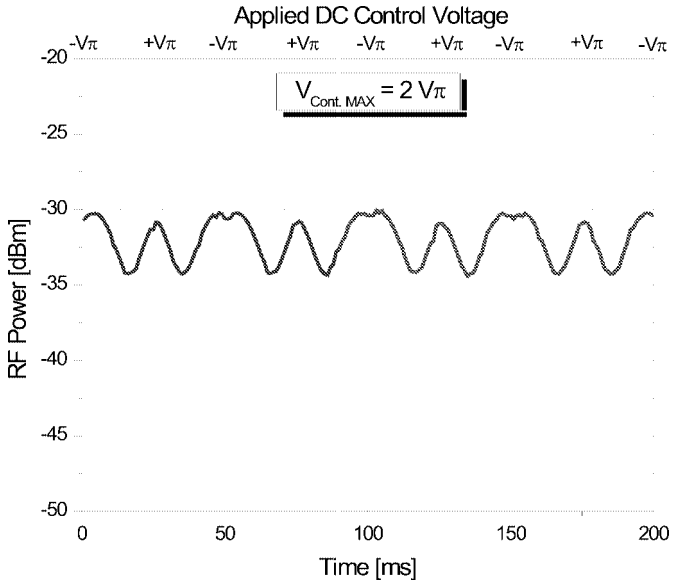

Fig. 8. The measured RF power from a single output.

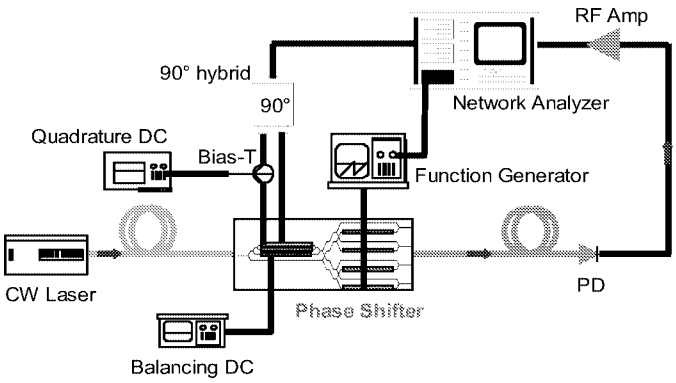

Fig. 9. The schematic diagram for the measurement setup.

For the control triangular waveforms of $2V_\pi(-12V \sim +12V)$, the RF phase was tuned by 360° with a high level of linearity, and the RF power varied by less than 4 dB, as expected from Figs. 2 and 3. Note that a single control of 360° of the RF phase shift corresponds to the half-cycle of the voltage change in triangular waveforms in time domain (25 ms). Accordingly, Figs. 7 and 8 represent eight times full operation within 200 ms. This performance can be even further improved by employing the design with the optional splitting ratio of the balancing arm, as described before.

These RF phase shifters should contain the most important feature that the RF phases of an array element are independently controlled. In order to confirm this, four triangular waveforms of $2V_\pi$, set by the equal time delays, were applied to the four dc control arms. The measured RF phase characteristics are shown in Fig. 10. Almost identical characteristics having the phase shift of 360° were observed for all output ports. It can be also seen from Fig. 10 that, at a given time frame, this arrangement results in the same effect generated by four different voltages and consequently introduces the independent phase shifts at four output ports. In addition, the independent control of the RF phase was also demonstrated by applying the

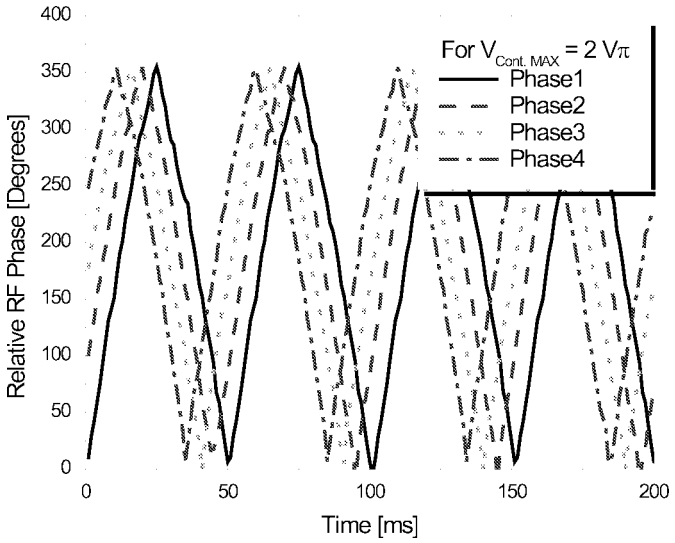

Fig. 10. The independently controlled four phase outputs introduced by equal delays on the triangular control voltages.

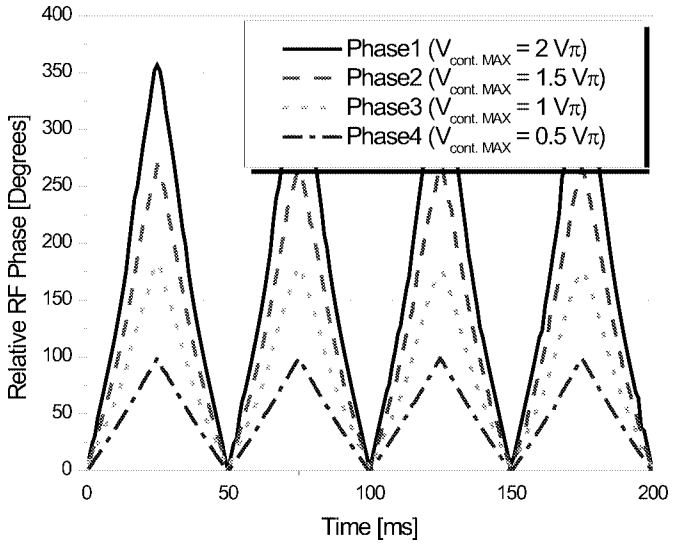

Fig. 11. The independently controlled four phase outputs introduced by the different triangular control voltages.

triangular waveforms having different peak-to-peak voltages to each control arm (Fig. 11).

The new generation of phase shifter is currently being developed, which can even reduce the complexity and drift from applying additional dc biases. Instead of using normal Y-junction splitting structures, two asymmetrical 1-by-2 MMI couplers can be used in front of the SSB modulator and the balancing arm, as shown in Fig. 12. These couplers will have multiple outputs and controllable phases depending upon their lengths and separations. This eventually will offer the built-in biases for the required optical phase shifts, removing the need for the quadrature dc biases of $V_{\pi/2}$ and V_{Bal}. Test devices of these MMI couplers were fabricated and measured. They showed the capability to provide the desired phases at two output ports. Therefore, these MMI integrated photonic RF phase shifters are expected to allow the simpler operation requiring only an RF feeding and control dc biases.

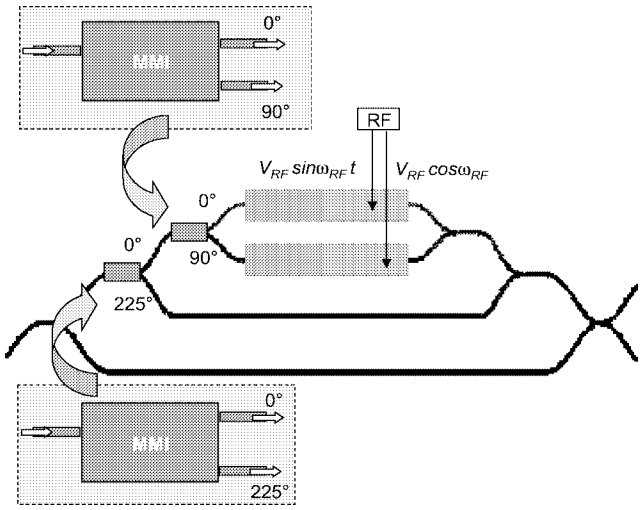

Fig. 12. The realization of the new generation of phase shifter structure incorporating MMI couplers.

IV. Conclusion

We have demonstrated a polymer-based four-element photonic RF phase-shifter array in a single chip. By employing a novel design to remove the operational drawbacks of this type of device, four phase outputs were independently controlled with high linearity and negligible power fluctuation. A simple vertical stack of these devices can now be used to form an $N \times N$ photonic RF phase shifter array without increasing complexity that will contribute to the future photonic phased array systems.

Acknowledgment

The authors would like to thank Dr. H. Erlig for valuable discussions.

References

[1] D. K. Paul, "Optical beam-forming and steering for phased-array antenna," in *Proc. IEEE Natural Telesys. Conf.*, June 1993, pp. 7–12.

[2] Y. Kamiya, W. Chujo, K. Yasukawa, K. Matsumoto, M. Izutsu, and T. Sueta, "Fiber optic array antenna using optical waveguide structure," in *IEEE Int. Symp. Dig. Antennas Propagation*, vol. 2072, May 1990, pp. 774–777.

[3] J. F. Coward, T. K. Yee, C. H. Chalfant, and P. H. Chang, "A photonic integrated-optic RF phase shifter for phased array antenna beam-forming application," *J. Lightwave Technol.*, vol. 11, pp. 2201–2205, Dec 1993.

[4] D. Jez, K. Cearns, and P. Jessop, "Optical waveguide components for beam forming in phased-array antennas," *Microwave Optical Technol. Lett.*, vol. 15, no. 1, pp. 46–49, 1997.

[5] J. M. Fuster, J. Marti, J. L. Corral, and P. Candelas, "Harmonic up/down-conversion through photonic RF phase shifters in phased-array antenna beam-forming applications," *Microwave Optical Technol. Lett.*, vol. 22, no. 4, pp. 247–249, Aug. 1999.

[6] S. R. Henion and P. A. Schulz, "Electrooptic phased array transmitter," *IEEE Photon. Technol. Lett.*, vol. 10, pp. 424–426, Mar. 1998.

[7] J. Han, H. Erlig, D. Chang, M. Oh, H. Zhang, C. Zhang, W. Steier, and H. Fetterman, "Multiple output photonic RF phase shifter using a novel polymer technology," *IEEE Photon. Technol. Lett.*, vol. 14, pp. 531–533, Apr. 2002.

[8] M. Oh, H. Zhang, A. Szep, V. Chuyanov, W. Steier, C. Zhang, L. Dalton, H. Erlig, B. Tsap, and H. Fetterman, "Electro-optic polymer modulators for 1.55 mm wavelength using phenyltetraene bridge chromophore in polycarbonate," *Appl. Phys. Lett.*, vol. 76, no. 24, pp. 3525–3527, 2000.

[9] S. Kim, H. Zhang, D. Chang, C. Zhang, C. Wang, W. Steier, and H. Fetterman, "Eelectrooptic polymer modulators with an inverted-rib waveguide structure," *IEEE Photon. Technol. Lett.*, vol. 15, pp. 218–220, Feb 2003.

[10] H. Nishihara, M. Harura, and T. Shhara, *Optical Integrated Circuits*. New York: McGraw-Hill, 1989.

Jeehoon Han (SM'01) received the B.S. degree in physics from Chonbuk National University, Chonju, Korea, in 1996 and the M.S. degree in electrical engineering from the University of Florida, Gainesville, in 1998. He is currently pursuing the Ph.D. degree in electrical engineering at the University of California, Los Angeles.

His work was on the fabrication of semiconductor laser devices. His current research is in the area of optoelectronic devices and optical communications using millimeter waves.

Byoung-Joon Seo received the B.S. degree in electrical engineering from Seoul National University, Seoul, Korea, in 1998. He is currently pursuing the M.S. degree at the University of California, Los Angeles.

He was with Woori Technology, Seoul, from 1998 to 2001.

SeongKu Kim was born on January 10, 1966, in KwangJu, Korea. He received the B.S. degree in electronics from the Chosun University, KwangJu, in 1989 and the M.S. and Ph.D. degrees in electrical engineering from Chonnam National University, KwangJu, in 1992 and 1996, respectively.

From 1994 to 1999, he was a Research Engineer with Korea Electronics Technology Institute, Seoul, Korea, where he developed the high-speed $LiNbO_3$ optical intensity modulators with a low optical loss and driving voltage. Since 2000, he has joined research programs in electrical engineering at the University of California, Los Angeles, where he initiated several projects involving the development of high-speed electrooptic polymer modulators and switches. His research interests are centered on high-speed fiber-optic communication devices, including electrooptic polymer and $LiNbO_3$ modulators and switches and their applications.

Hua Zhang, photograph and biography not available at the time of publication.

Harold R. Fetterman received the B.A. degree (with honors) from Brandeis University, Waltham, MA, in 1962 and the Ph.D. degree from Cornell University, Ithaca, NY, in 1968, both in physics.

He joined Lincoln Laboratory in 1969, where his initial research concentrated on the use of submillimeter sources for spectroscopy. In 1982, he joined the Electrical Engineering Department of the University of California, Los Angeles, as a Professor and served as the first Director of the Center for High Frequency Electronics. He has concentrated on combining high-frequency structures and systems with optical devices. These efforts include continuous-wave optical mixing experiments using three terminal devices, high-speed polymer optical modulators, and traveling-wave photodetectors, which are now being extended to over 200 GHz. Some of these devices have been incorporated into novel systems such as optically controlled phased array radars and, more recently, new forms of optical A-to-Ds.